Fractionation of Poly(ethylene-*co*-vinyl acetate) in Supercritical Propylene: Towards a Molecular Understanding of a Complex Macromolecule

B. FOLIE,[1] M. KELCHTERMANS,[2] J. R. SHUTT,[1] H. SCHONEMANN,[3] V. KRUKONIS[3]

[1] Exxon Chemical Company, Baytown Polymers Center, PO Box 5200, Baytown, Texas 77522-5200

[2] Exxon Chemical Europe, Machelen Chemical Technology Center, Hermeslaan 2, B-1831 Machelen, Belgium

[3] Phasex Corporation, 360 Merrimack Street, Lawrence, Massachusetts 01843

Received 7 August 1996; accepted 20 November 1996

ABSTRACT: A commercial low-density polyethylene copolymer, poly(ethylene-*co*-vinyl acetate) (EVA), synthesized via the high-pressure free-radical polymerization process, was fractionated with supercritical propylene by isothermal increasing pressure profiling and critical, isobaric, temperature rising elution fractionation (CITREF™). Extensive characterization of the fractions by nuclear magnetic resonance (NMR) spectroscopy, gel permeation chromatography (GPC) in combination with low-angle laser light scattering (LALLS), and differential scanning calorimetry (DSC) was used to map not only the molecular-weight and chemical composition distributions of the parent copolymer, but also its short-chain branch (SCB) and long-chain branch (LCB) distributions. Fractionation by increasing pressure profiling confirmed the broad molecular-weight distribution and the narrow acetate-branch distribution expected for this random copolymer but revealed the presence of a small amount (~ 2 wt %) of low molecular-weight amorphous species containing a high level of alkyl SCBs (80 branches/1000 C). The LCB density estimated from the Zimm–Stockmayer relationship using the GPC data monotonically increases with increasing molecular weight above 60,000 g/mol, in agreement with the kinetics of free-radical polymerization. CITREF™ was found to fractionate this copolymer by crystallinity, which is influenced by both the alkyl SCBs and the acetate branches. Up to 18% difference in total branch density ($<5\%$ in crystallinity) between EVA molecules was identified using CITREF™. © 1997 John Wiley & Sons, Inc. J Appl Polym Sci **64:** 2015–2030, 1997

Key words: supercritical fractionation; isothermal increasing pressure profiling fractionation; critical, isobaric, temperature-rising elution fractionation (CITREF™); high-pressure poly(ethylene-*co*-vinyl acetate) (HP-EVA)

INTRODUCTION

Increased interest in determining polymer properties, evaluating reaction kinetics and catalyst performance, producing new polymer products, and obtaining gel permeation chromatography (GPC) standards have been the motivation for the development of processes to fractionate polymers. Polymer fractionation has been used traditionally to determine the detailed molecular architecture of semicrystalline ethylene-based homo- and copolymers, including their molecular-weight distribution (MWD), branching distribution, and chemical composition distribution (CCD). The

Correspondence to: B. Folie.

 CCC 0021-8995/97/102015-16

most popular techniques are liquid antisolvent fractionation and GPC fractionation, which separate molecules with respect to size at temperatures above the melting point of the polymer in solution, and temperature-rising elution fractionation (TREF), which separates them with respect to crystallinity at temperatures below the polymer crystallization temperature.[1,2] There are practical drawbacks to these techniques; e.g., they typically require large amounts of liquid organic solvents, and they produce only very small (mg) quantities of material.

Recently, there has been a growing interest in using supercritical fluid (SCF) solvents to fractionate polymers with respect to size, chemical composition, and backbone architecture (branchiness). The ability of SCF solvents to fractionate polymers is due to their pressure-dependent dissolving power in combination with their ability to discriminate in any homologous series by molecular weight (MW).[1,2] SCF fractionation of polymers has been shown to be a relatively rapid technique that provides multigram-sized fractions of narrow MWD and/or narrow CCD.[1,2] An overview of the principles underlying supercritical fractionation of polymers is found in the treatise by McHugh and Krukonis[2] and in a recent review article by McHugh et al.[1]

Among the techniques used for fractionating polymers with SCFs, isothermal increasing pressure profiling has been used to fractionate ethylene-based copolymers with respect to MW. For instance, Saltzman et al.[3] fractionated a high-pressure poly(ethylene-*co*-vinyl acetate) (HP-EVA) in supercritical propane, resulting in narrow MWD fractions of increasing MW but of the same vinyl acetate (VA) content. Pratt et al.[4] and McHugh[5] also used that technique to fractionate a series of poly(ethylene-*co*-methyl acrylate) (EMA) and poly(ethylene-*co*-acrylic acid) (EAA) copolymers with respect to chemical composition using, sequentially, several SCF solvents of increasing polarity. Ehrlich[6] and Watkins et al.[7] were the first to demonstrate the use of critical, isobaric, temperature-rising elution fractionation (CITREF™), a supercritical variant of TREF, to fractionate a high-density polyethylene (HDPE) with respect to the polymer backbone architecture, i.e., its alkyl short-chain branch (SCB) density, using supercritical propane.

In this work, a commercial HP-EVA containing 11 mol % incorporated VA was fractionated with supercritical propylene by isothermal increasing pressure profiling and CITREF™. To our best knowledge, this is the first time that CITREF™ has been applied to the fractionation of an ethylene-based copolymer. Extensive characterization of the fractions by nuclear magnetic resonance (NMR) spectroscopy, gel permeation chromatography (GPC) in combination with low-angle laser light scattering (LALLS), and differential scanning calorimetry (DSC) was used to map, not only the MWD and CCD of the parent copolymer but also its SCB and long-chain branch (LCB) distributions. The in-depth characterization of the fractions performed in this work resulted in a more fundamental understanding of the molecular architecture of that complex macromolecule and provided new insights on the kinetics of free-radical polymerization at high pressure.

EXPERIMENTAL

Polymer Fractionation: Equipment and Techniques

A schematic diagram of the dynamic flow apparatus used for the isothermal increasing pressure profiling fractionation and CITREF™ is shown in Figure 1; the system can operate at conditions of 200°C and 700 bar. During typical operation of a fractionation test, the SCF solvent is compressed by a diaphragm compressor (Newport Scientific) to a desired pressure controlled by a back pressure regulator (Tescom Corporation). The compressed gas is delivered at a flow rate of about 20 L/min (STP) to a surge tank/preheater in series with the extraction column (240 mL; 1.7 cm i.d. $\times$ 100 cm length). The column contains a dense knitted stainless steel mesh packing (Goodloe®), which serves as a high surface area support for the molten polymer. Pressure is controlled to within ± 5 bar, and the flow rate controlled via a pressure-reduction valve. The temperature of the extraction column is maintained to within ± 1°C, as measured by one thermocouple located near the exit of the column; another thermocouple located on the skin of the vessel controls the column temperature. Downstream of the extractor, the SCF solvent, laden with dissolved polymer extracted from the charge, is expanded to atmospheric pressure via the pressure reduction/heated valve. The precipitated polymer fraction is collected in a preweighted U-tube. A glass-wool filter at the exit of the U-tube is used to trap any fine particles entrained in the gas. The ambient SCF solvent passes through a flowmeter (Fischer-Porter) and a dry test meter (Singer) to measure, respectively,

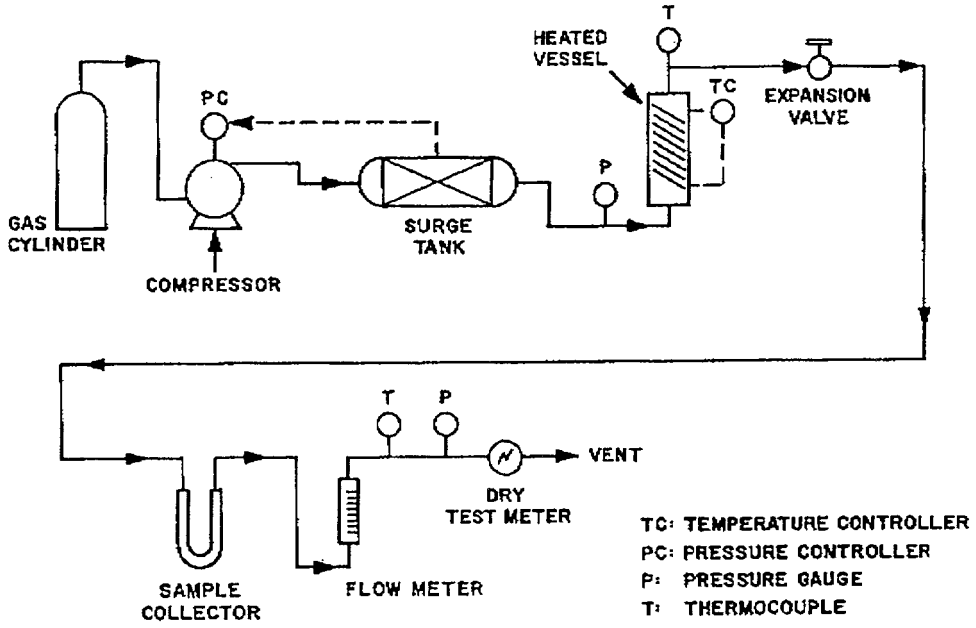

Figure 1 Schematic diagram of the fractionation equipment used in this work.

the instantaneous flow rate and the total volume passed through the extractor.

Propylene, a moderately polar solvent, was chosen as the SCF solvent for this weakly polar EVA containing approximately 11 mol % VA. The choice of this particular SCF solvent follows from the recommendations made by Pratt et al.[4] to match the physical properties of the SCF solvent with those of the polymer to insure a finite solute solubility at the conditions of the fractionation. However, the resulting favorable solute-solvent interactions should not overwhelm the effect of the solvent density, which, at a temperature above the melting point of the polymer, remains the key parameter to fractionate polymers by the isothermal increasing pressure profiling technique. In other words, the cloud point pressure (CPP) of the polymer-SCF solution at the selected fractionation temperature should be high enough so that increasing the pressure stepwise during the isothermal increasing pressure profiling fractionation will cause the solvent density to be varied sufficiently, but the CPP should also be low enough to allow the complete dissolution of the parent polymer to occur in the apparatus. Given the above two criteria, propylene was selected as the SCF solvent based on the CPP data reported[4] for a propylene solution containing $\sim$ 5 wt % EMA, a LDPE copolymer structurally and chemically similar to the parent EVA used in this work; the CPP of EMA was measured to lie around 500 bar over the range of 85–140°C, and these conditions are well within the design limits of the apparatus used in this study.

Fractionation by Size: Isothermal Increasing Pressure Profiling

Isothermal increasing pressure profiling is a well-known technique using SCFs to fractionate polymers by size into fractions of narrow MWD.[1] This technique is explained in detail elsewhere.[2] Briefly, for the test, 9.75 g of EVA pellets (3 mm in diameter) was charged to the extraction vessel and dispersed over the dense stainless steel knitted mesh. The vessel was sealed and pressurized to 136 bar with propylene. The temperature of the vessel was then brought to 120°C, a temperature well above the melting point of the polymer, resulting in a thin polymer-rich coating, evenly spread on the packing. The polymer was fractionated isothermally by ramping the pressure in increments of 10 to 20 bar, from 136 bar to a final pressure of 530 bar. At each selected pressure level, the propylene flow through the extraction column was continued until the amount of extract collected at the U-tube became imperceptible. The solvent flow was then stopped, a new U-tube attached, and the pressure raised to the next level. In principle, the MWD of the fractions can be made as narrow as desired based upon the number of fractions (pressure levels) collected. Twenty-five fractions were collected in this work.

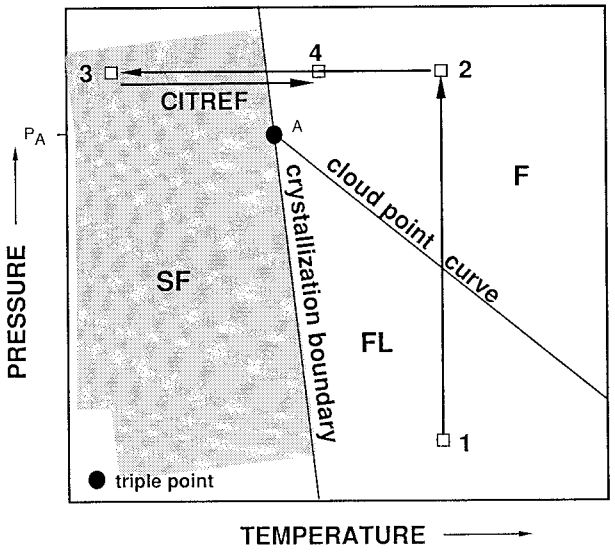

Figure 2 Qualitative isopleth P-T phase diagram typical for semicrystalline polymer-SCF systems, showing the three steps used in CITREF™.

Fractionation by Crystallinity: Critical, Isobaric, Temperature-rising Elution Fractionation

As described previously,[6,7] CITREF™ has been used to fractionate semicrystalline HDPE based on crystallinity, which depends solely on the alkyl SCB density; it is used here, for the first time, to fractionate a LDPE copolymer whose crystallinity depends on both the alkyl SCB-density and the acetate-branch density. The steps used to carry out CITREF™ are illustrated in the qualitative pressure-temperature (P-T) isopleth diagram shown in Figure 2 for a typical semicrystalline polymer-SCF system.[8] Steps 1–2 and 2–3 in Figure 2 constitute the recrystallization part of CITREF™, i.e., the sample preparation steps; step 3–4 denotes the fractionation path. For the test, the extraction vessel was charged with 13.08 g EVA, heated to 85°C, and pressurized to 612 bar with propylene. At that pressure and temperature, which correspond to point 2 in Figure 2, the polymer-SCF system consists of a single, homogeneous fluid phase (F), well above its CPP at 85°C. Note that the pressure at point 2 should also lie above P_A, the pressure corresponding to point A in Figure 2, in order to prevent the formation of a polymer-rich liquid phase (L) during cooling. Point A is a triple point where three phases, solid-fluid-liquid (SFL), coexist.[8] The system was kept at the above conditions (85°C/612 bar) for six hours under buoyancy mixing to ensure complete dissolution of the polymer and uniform concentration in the vessel. The polymer solution was then cooled isobarically at a rate of 5°C/h down to −1°C, a temperature well below the crystallization temperature of the parent polymer. The polymer was deposited onto the packing by this procedure. The recrystallization of the polymer from solution, shown as step 2–3 in Figure 2, serves two purposes, both of which contribute to minimize mass transfer limitations (polymer accessibility) during the subsequent fractionation. First, it causes the polymer to be deposited as a thin semicrystalline layer on the high surface area support; and second, the isobaric decreasing temperature path is itself a continuous fractional crystallization with the most crystalline (highest melting temperature) material deposited first and the least crystalline (lowest melting temperature) material deposited last on the support; the least crystalline material is, thus, readily accessible as CITREF™ commences.

After the recrystallization step was completed, the polymer was fractionated isobarically by ramping the temperature in 4°C increments to a final temperature of 54°C (step 3–4 in Fig. 2), at which temperature all the copolymer had been dissolved and extracted. Note that the amorphous portion of the charge remains dissolved in propylene during the deposition step and is eluted with the first fraction. As for the pressure profiling fractionation, the flow of propylene was maintained at each selected temperature until the amount of extract collected in the U-tube became imperceptible. Fourteen fractions were collected in this study.

Polymer Characterization: Equipment and Techniques

The 25 EVA fractions obtained from the isothermal increasing pressure profiling fractionation, the 14 EVA fractions obtained from CITREF™, and the parent EVA were characterized by NMR, GPC, and DSC, as described in detail below. The characterization results for the parent EVA are summarized in Table I.

Nuclear Magnetic Resonance Spectroscopy

NMR spectra were determined at 125°C on a Varian Unityplus 300 MHz instrument. The ^{1}H-NMR spec-

Table I Characterization Results of the Parent EVA

Property	Measured Value	Units	Method
M_w	136,800	g/mol	GPC-LALLS
M_n	25,300	g/mol	GPC-DRI
PD	5.41	—	GPC-DRI/LALLS
LCB factor, g'_{II}	0.424	—	GPC-DRI/LALLS
n_w	22.75	LCB/molecule	GPC-DRI/LALLS
LCB density	2.33	LCB/1000 C	GPC-DRI/LALLS
Alkyl density	9.29	branch/1000 C	^{1}H-NMR
Acetate density	48.45	branch/1000 C	^{1}H-NMR
T_m (peak)	74.22	°C	DSC
T_c (peak)	53.70	°C	DSC
ΔH_f	38.53	J/g	DSC
ΔH_c	−40.89	J/g	DSC
% Crystallinity[a]	13.6	%	DSC

[a] % Crystallinity = $(\Delta H_f/\Delta H_f^o) \times 100$, where ΔH_f^o is the enthalpy of fusion of a single polyethylene crystal.

tra were obtained using a 5 mm probe on ±5 wt % polymer solutions in 1,2,4-trichlorobenzene/deuterobenzene mixtures (80 : 20 volume ratio). The spectra are referenced to the CH_2 peak at 1.3 ppm. Based on these ^{1}H-NMR spectra, the mole percent incorporated VA (1 H at 4.95 ppm) was determined. Also, the number of methyl groups (3 H at 0.95 ppm) per 1000 carbons (later referred to as the alkyl-branch density) and the number of acetate groups (1 H at 4.95 ppm) per 1000 carbons (later referred to as the acetate-branch density), including the acetate groups at the chain end (1 H at 4.45 ppm), were calculated. Note that the alkyl-branch density obtained by ^{1}H-NMR includes the methyl groups on saturated carbons arising from the SCBs, the LCBs, and the saturated chain ends, as well as those introduced by the free-radical initiator, the chain transfer agent, etc. Similarly, the acetate-branch density includes both the acetate groups per se and those acetate groups whose methyl groups have undergone further reaction, resulting in a LCB off the acetate group. The number of such acetate groups was also estimated in this work (2 H at 2.35 ppm) and was found to represent less than 1% of the total acetate branch density in this particular EVA. The different types of branches that are typically present in HP-EVA are illustrated in Figure 3.

As was pointed out earlier, the methyl group of the incorporated acetate groups is susceptible to hydrogen abstraction because a mesomerically stabilized radical is formed. This radical can then further add monomers, generating a LCB off the acetate group. Radical stabilization also explains why there is no branch generated on the methine group carrying the incorporated acetate group. In the later case, hydrogen abstraction would generate a radical that is inductively destabilized by the adjacent electron-withdrawing oxygen. These two mechanisms are illustrated here below.

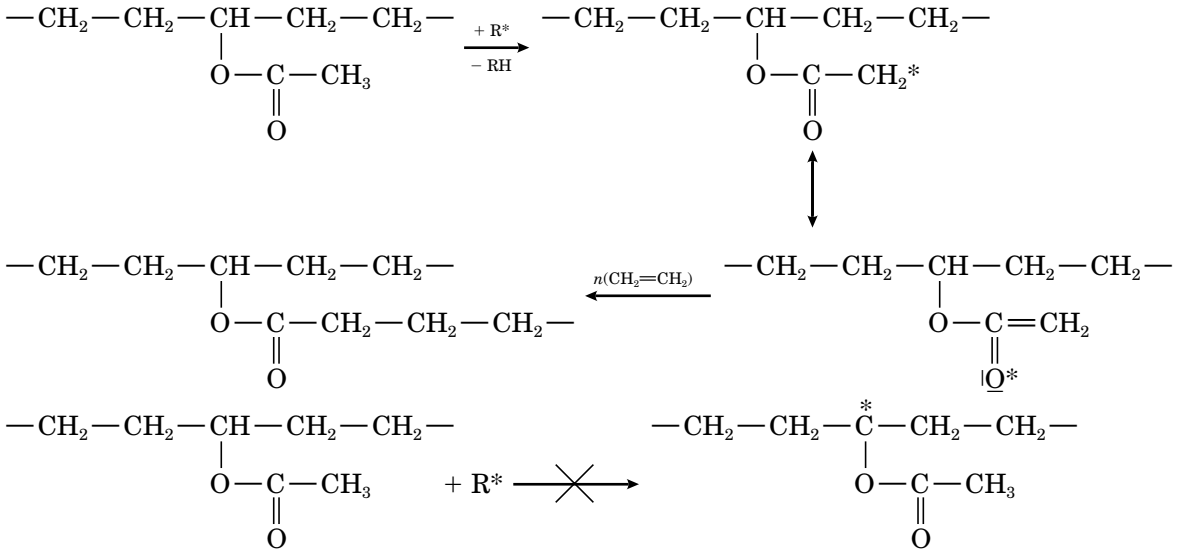

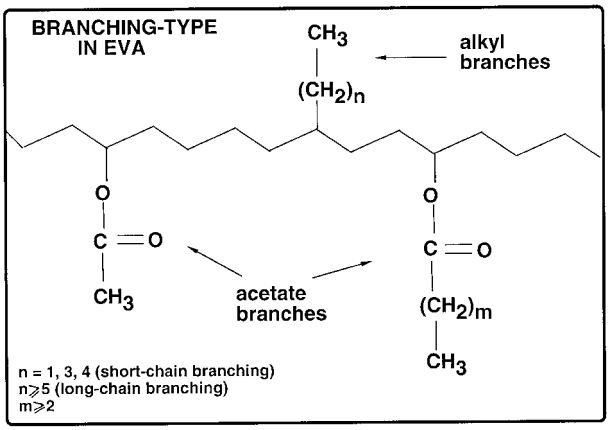

Figure 3 Schematic diagram of the different types of branches typically encountered in HP-EVA.

On the other hand, branching off the backbone carbon carrying the functional group has been observed with other ethylene copolymers,[9] such as poly(ethylene-*co*-acrylonitrile), poly(ethylene-*co*-butyl acrylate), EAA, and EMA. In addition, for these copolymers, branching off the backbone carbon carrying the functional group can also occur by intramolecular chain transfer.[9]

The ^{13}C-NMR spectra were also obtained at 125°C on the same instrument using a 10 mm probe on ±15 wt % polymer solutions in 1,2,4-trichlorobenzene/deuterobenzene mixtures (80 : 20 volume ratio). These spectra are referenced to the CH_2-$\delta^+\delta^+$-peak at 29.9 ppm. This technique allows a determination to be made of the number of alkyl branches of different sizes per 1000 carbons: ethyl (between 12 and 6 ppm), butyl (at 23.4 ppm), amyl (at 32.9 ppm), and hexyl+ (at 32.2 ppm). Note that the hexyl+ includes the LCBs and the paraffinic chain ends.

Gel Permeation Chromatography

GPC was performed at 135°C on a Waters 150-C ALC/GPC, equipped, on-line, with a Waters Differential Refractive Index (DRI) detector and a LDC Analytical Chromatix KMX-7 LALLS detector. The samples were prepared at a concentration of 3.5 mg per mL in 1,2,4-trichlorobenzene. HPLC-grade 1,2,4-trichlorobenzene, to which 0.1 vol % of polyethylene glycol was added, was used as the eluting solvent (0.5 mL/s). The polymer molecules are separated according to their hydrodynamic volume over four Shodex columns, packed with styrene-divinylbenzene gels (with exclusion limits for polystyrene from 5000 to 5,000,000 g/mol). The refractometer was calibrated with NBS-1475 (linear polyethylene), and the calibration curve corrected for the presence of 11 mol % incorporated VA. In general, GPC-DRI provides good estimates of the weight-average MW (M_w), of the number-average MW (M_n), and of the polydispersity (PD = M_w/M_n) of linear polymers, but the technique underestimates the MWs of branched polymers. GPC-LALLS, on the other hand, provides absolute MWs. Neglecting the second virial coefficient ($A_2 = 0$), the scattering signal (S_ϕ with $\phi = 5$ degrees) measured at each retention volume u is directly related to the polymer molecular weight $M(u)$,

$$S_\phi(u) = k[c(u)M(u)] \tag{1}$$

where $c(u)$ is the polymer concentration measured by the refractive index detector, and k is an optical constant related to $(dn/dc)^2$, with (dn/dc) being the change in index of refraction with polymer concentration. M_w can be estimated rigorously by integrating the LALLS-signal (S_ϕ), as follows:

$$M_w = \frac{\int S_\phi(u)du}{kc_0V_0} \tag{2}$$

where c_0 is the whole sample concentration (2.5 to 5.0 mg/mL), and V_0 is the injection volume (120 μL). M_n, on the other hand, must be estimated from the differential MWD reconstructed from

$$W[\log M(u)] = \frac{c(u)}{(d \log M(u)/du)} \tag{3}$$

where $W[\log M(u)]$ is the amount of polymer contained between $\log M(u)$ and $[\log M(u) + d \log M(u)]$, and $d \log M(u)/du$ is obtained from a polynomial fit of the $\log M(u)$ versus u data calculated from eq. (1).[10] Note that since the LALLS signal is proportional to $\sim cM$ [eq. (1)], it was found to be too weak to estimate M_n reliably; hence, M_n determined from GPC-DRI and M_w determined from GPC-LALLS are used to estimate the polydispersity of the fractions in this work. The MWDs obtained from GPC-DRI and GPC-LALLS are compared for the parent EVA and the highest MW fraction (#25) obtained from isothermal increasing pressure profiling in Figures 4(a) and 4(b), respectively. In both cases, the MWD determined by GPC-LALLS is shifted towards higher MW, indicating the presence of branched molecules in those samples.

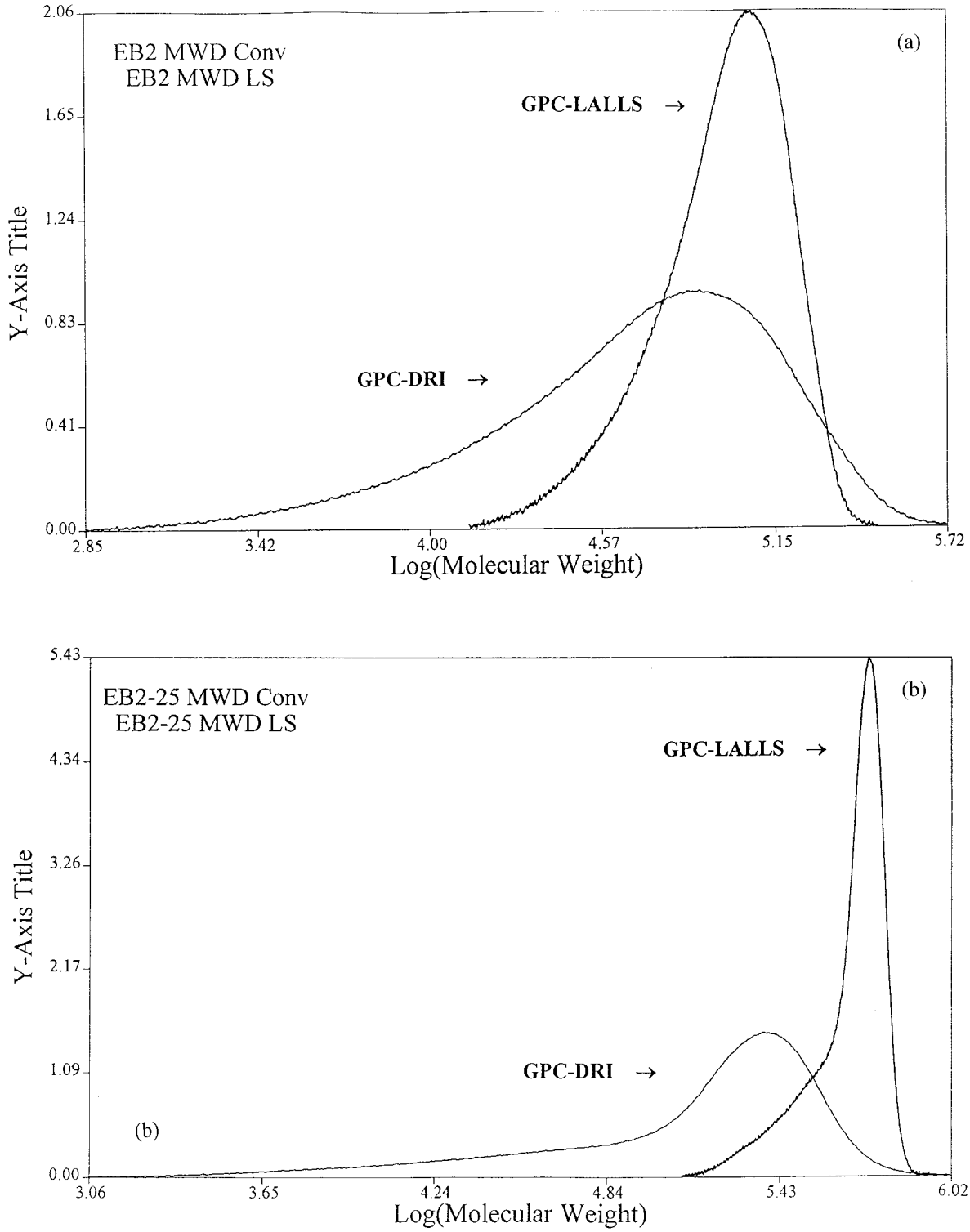

Figure 4 The MWDs obtained from GPC-DRI and GPC-LALLS for (a) the parent EVA and (b) the highest MW fraction (#25) obtained from isothermal increasing pressure profiling.

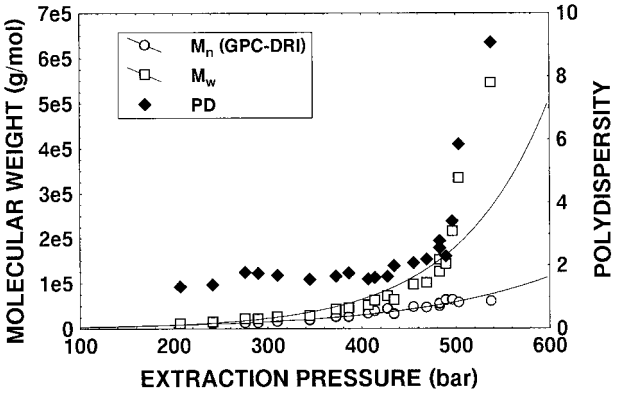

Figure 5 Relationship between the average MWs and the polydispersity of the fractions obtained from isothermal increasing pressure profiling and the extraction pressure.

Differential Scanning Calorimetry

DSC was performed on a Perkin Elmer DSC-7, calibrated with indium for temperature and enthalpy of fusion. About 5 mg of polymer is typically used in each DSC test. To eliminate any effect of thermal history, the sample is first subjected to a heating cycle from 0 to 190°C at a rate of 10°C per minute. After keeping the samples two minutes at 190°C, the sample is subjected to a cooling cycle at a rate of 10°C per minute, during which the crystallization temperature (T_c) is recorded and the crystallization enthalpy (ΔH_c) determined. Last, after holding the sample for two minutes at 0°C, the sample is subjected to a second heating cycle to determine melting temperature (T_m) and enthalpy of fusion (ΔH_f).

RESULTS AND DISCUSSION

EVA Fractionation by Isothermal Increasing Pressure Profiling

Figure 5 shows the relationship between the extraction pressure and the MW of the 25 fractions obtained from isothermal increasing pressure profiling. As expected, both M_w and M_n determined from GPC-LALLS and GPC-DRI, respectively, steadily increase with increasing pressure because of the increasing density, hence, dissolving power, of propylene with pressure. Isothermal increasing pressure profiling is known to generate fractions with narrow MWDs, in other words, with small polydispersities.[1,2] The MWDs (obtained from GPC-DRI) of eight selected fractions and the parent EVA are shown in Figure 6. As expected, the MWDs of the fractions are considerably narrower than the MWD of the parent EVA. Note, however, than the MWDs become progressively broader towards the high MW end of the spectrum. As shown in Figure 5, the polydispersity is small and nearly constant ($\sim 1.5 < \text{PD} < \sim 2.0$) up to about 450 bar and then increases rapidly with increasing pressure. This abrupt increase in the polydispersity can be explained by the following two arguments: 1) as the extraction pressure increases, the dissolving power of the SCF solvent also increases, which lowers its selectivity, making it capable of solvating molecules of more different sizes,[11] and 2) as it is explained in details below, the concentration of LCBs rapidly increases with increasing MW in this copolymer, which affects M_w to a greater extent than M_n. Note that the polydispersities of the high MW fractions shown in Figure 5 represent upper values since M_n obtained from GPC-DRI is probably slightly underestimated for those fractions containing branched chains.

Figure 7 shows the results of the ^{1}H-NMR analyses of the respective fractions. The acetate, alkyl, and total branch densities (expressed as number of branches per 1000 total carbon atoms) are shown as a function of $\log_{10}(M_w)$. Whereas the acetate branch density is nearly constant in all the fractions collected ($\sim$ 45 acetate branches/1000 C), the data indicate that the alkyl branch density rapidly increases with decreasing MW for $M_w < 20{,}000$ g/mol. In fact, the alkyl branch density of the lowest MW fraction ($\sim$ 80 alkyl branches/1000 C) is nearly ten times that of the high MW fractions ($\sim$ 8 alkyl branches/1000 C); as a result, the total branch density (alkyl + acetate) of the lowest MW fraction is more than twice ($\sim$ 125 branches/1000 C) that of the high MW fractions. There was no melting or crystallization peak detected by DSC for the first two fractions, indicating that those fractions are fully amorphous as a result of their high total branch density. Similar trends were found by Wild et al.,[12] who observed, by cross-fractionating fractions obtained from preparative TREF by SEC, relatively narrow but strongly MW-dependent SCB distributions in HP-LDPE, with the lower MW species being the more branched. Similarly, Shirayama et al.[13] found that the SCB distribution in HP-LDPE becomes broader as the average MW of the fractions decreases.

EVA is produced commercially by free-radical azeotropic copolymerization at high pressures

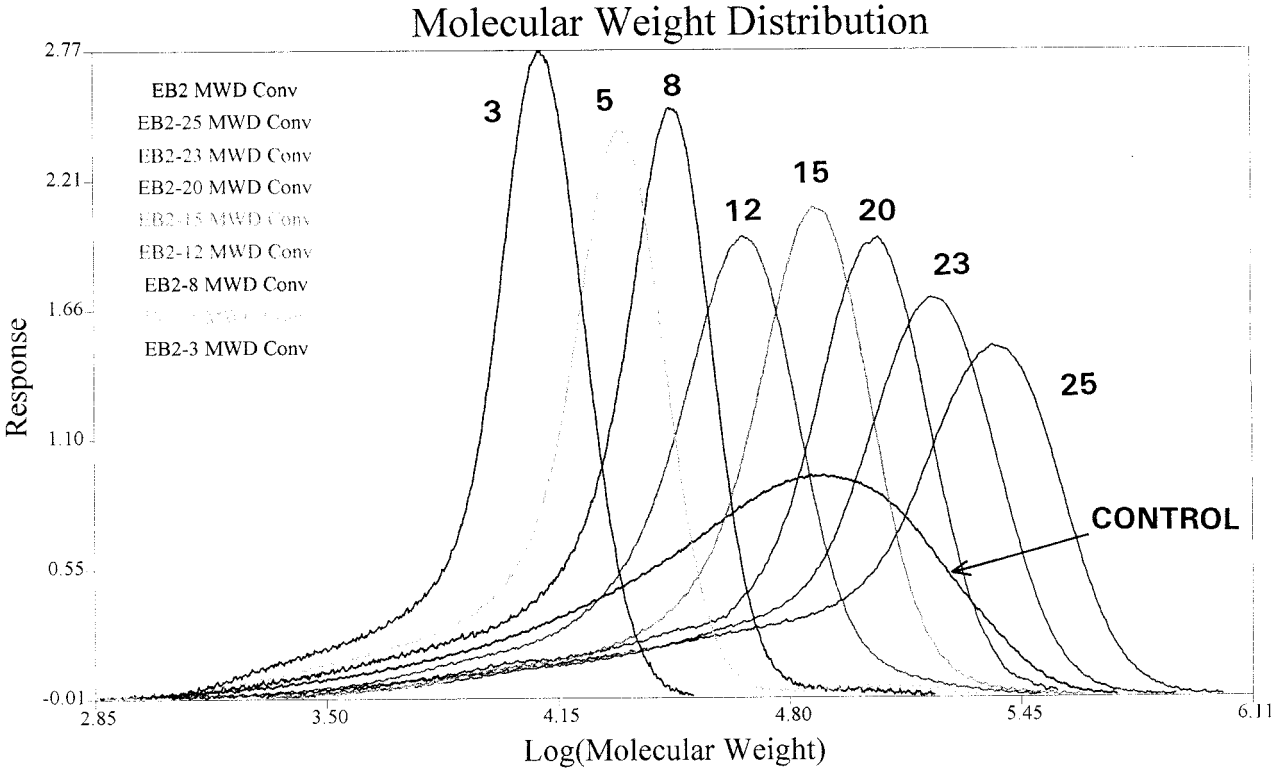

Figure 6 The MWDs obtained from GPC-DRI for eight selected fractions and the parent EVA (labeled control).

(1500–3000 bar). Since the reactivity of ethylene and VA is very similar in HP free radical polymerization as indicated by the fact that both reactivity ratios are close to one ($r_1 = r_2 = \sim 1.0$),[14] VA is not only randomly distributed along the chains ($r_1 r_2 = \sim 1.0$), but also the average VA content of the fractions is independent of their average MW since the VA to ethylene molar ratio remains constant along the staged autoclave reactor. On the other hand, according to Stockmayer's bivariate distribution,[15] one would expect a broadening in CCD as the average MW of the fractions decreases. In general, commercial HP-EVAs are characterized by a broad MWD but a narrow CCD. The latter trend is also confirmed by the data of Saltzman et al.[3] The broad MWD but the narrow alkyl branch density distribution and CCD characteristic of this EVA are illustrated by the cumulative weight distributions shown in Figure 8(A)–(C).

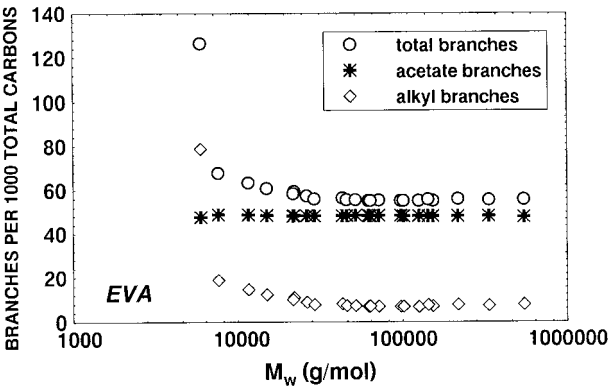

Figure 7 Number of branches per 1000 total carbons as measured by ^{1}H-NMR shown as a function of $\log_{10}(M_w)$ for the fractions obtained from isothermal increasing pressure profiling.

Fractionating of EVA in supercritical propylene by isothermal increasing pressure profiling yields a small fraction (~ 2 wt %) of highly branched and amorphous low MW species. Those alkyl branches are essentially SCBs, which result from intramolecular back-biting (via the Roedel mechanism[14]) in free radical polymerization. The particular EVA fractionated in this study was synthesized in a HP autoclave reactor using a split temperature profile mode, with the reactor bottom temperature 40°C higher than the top temperature. It is likely that the highly branched

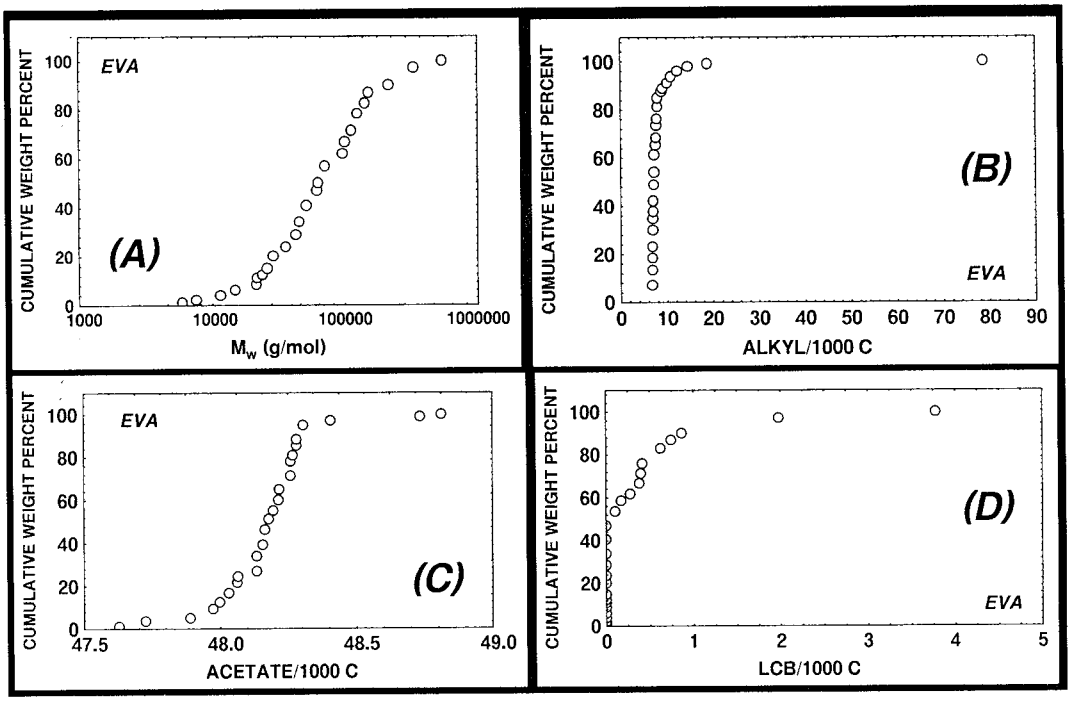

Figure 8 The cumulative weight distributions reconstructed from the fractions obtained by isothermal increasing pressure profiling for (A) M_w, (B) the alkyl branch density, (C) the acetate branch density, and (D) the LCB density.

low MW species are made late in the reaction scheme at the high-temperature end. As shown by Feucht et al.,[16] short-chain branching is favored by high temperatures but is nearly independent of residence time and initiator concentration in HP autoclave reactors.

Shown in Figure 9 are the DSC melting temperature T_m and the DSC crystallization temperature T_c for fractions #3 to #25 plotted versus M_n. These data confirm the fact that, at nearly constant branch density, the polymer density and crystallinity are also functions of the polymer MW. Indeed, the data of Figure 9 indicate that the lower MW species crystallize to a greater extent, with T_m and T_c of the fractions increasing with decreasing M_n. These trends were not expected since it is well known that T_m for linear PE crystallized from solution decreases with decreasing MW in the lower MW region (<10,000 g/mol), the chain ends acting as noncrystallizable units, while T_m becomes nearly independent of MW above 10,000 g/mol.[12] The data shown in Figure 9 indicate that when the polymer is crystallized from the melt, T_m exhibits a significant MW dependence, even for MW > 10,000 g/mol. One can speculate that the crystallizability of the chains in the melt is controlled by the chain mobility, hence, by the extent to which they can pack closely to form lamellae, which should favor the more mobile, lower MW species.

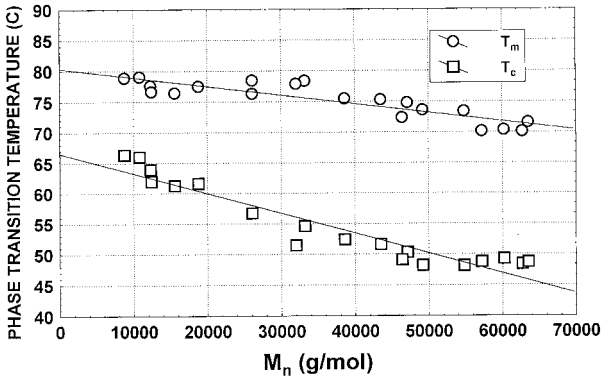

Figure 9 The polymer melting temperature (T_m) and crystallization temperature (T_c), as determined by DSC, shown as function of M_n.

Long-chain Branching

LDPE is known to be made of nonlinear (dendritic) chain molecules containing a variable amount of LCBs resulting from intermolecular chain transfer.[14] As was pointed out earlier, GPC-

DRI separates macromolecules according to their hydrodynamic volume (V_H). The MWs obtained from GPC-DRI are therefore accurate only for linear chain molecules for which, in a dilute solution, V_H is related to M, the chain MW, according to

$$V_H \propto R_g^3 \propto [\eta]M \propto M^{(1+\beta)} \tag{4}$$

where R_g is the mean radius of gyration of the chain, and β is 0.5 for θ-solvents and $\sim$ 0.8 for good solvents. The MWs obtained from GPC-DRI are typically underestimated for branched molecules, such as HP-LDPE, because the elution volume of a branched molecule corresponds to a linear molecule with a lower apparent MW. If LALLS is used online with GPC-DRI, the absolute MW of the polymer can be measured continuously, regardless of the polymer branchiness. Following Zimm and Stockmayer,[17] the ratio of the intrinsic viscosity of a branched polymer, $[\eta]_{branched}$, to that of a linear polymer of equal composition and MW, $[\eta]_{linear}$, is directly related to the degree of LCB in the branched polymer, expressed here as the LCB factor, g'_H. Assuming that the universal calibration is valid, g'_H can be estimated from measurable MWs by the following expression[18]:

$$g'_H \equiv \frac{[\eta]_{branched}}{[\eta]_{linear}} \cong \left(\frac{M_w^*}{M_w}\right)^{\alpha+1} \tag{5}$$

where M_w^* is the MW of a linear molecule with the same elution volume, estimated here from GPC-DRI; M_w is the absolute M_w of the branched polymer determined by GPC-LALLS; and α is the exponent for the corresponding linear polymer in the Mark–Houwink relationship $[\eta] = K(M_v)^\alpha$, where $K = 4.06 \times 10^{-4}$ dL/g and $\alpha = 0.725$ for polyethylene in TCB at 135°C. The LCB density for each fraction can be computed by estimating the LCB factor g, which is defined as the ratio of the mean radii of gyration of the same polymers and is related to g'_H by[18]

$$g \equiv \frac{[R_g^2]_{branched}}{[R_g^2]_{linear}} \cong (g'_H)^{1/B} \tag{6}$$

where B is a constant related to the type and amount of branching, which typically ranges between 0.5 and 1.5 for polyethylene.[18] An average value of 0.65 for B, as recommended by Mirabella and Wild[19] for LDPE in the LCB/1000 C range of 0 to 10, was used in this work. For polydisperse polymers with trifunctional branch points, g ($= \langle g \rangle_w$) is in turn related to n_w, the weight-average number of branches per molecule by[17]

$$\langle g \rangle_w = \frac{6}{n_w}\left\{\frac{1}{2}\left(\frac{2+n_w}{n_w}\right)^{1/2} \times \ln\left[\frac{(2+n_w)^{1/2}+n_w^{1/2}}{(2+n_w)^{1/2}-n_w^{1/2}}\right]-1\right\} \tag{7}$$

from which the LCB density can be easily estimated from

$$\frac{\text{LCB}}{1000C} = \frac{14{,}000\ n_w}{M_w} \tag{8}$$

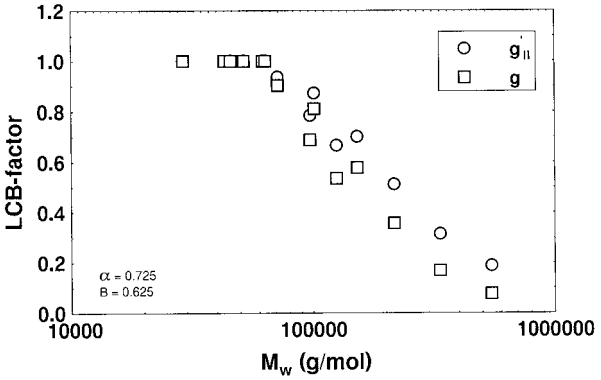

Figure 10 The LCB factors g'_H and g, shown as a function of $\log_{10}(M_w)$. Both LCB factors rapidly decrease below 1.0 as the extraction pressure is raised above $\sim$ 450 bar, indicative of a steady increase in LCB content with increasing M_w above 60,000 g/mol.

g'_H and g are used to estimate qualitatively the degree of branching of each EVA fraction. The results are presented in Figure 10, where g'_H and g are shown as a function of $\log_{10}(M_w)$. As shown in Figure 10, g'_H and g are nearly equal to 1.0 up to about 60,000 g/mol, indicating that the low MW fractions are made of nearly linear chains containing few LCBs. At $M_w > 60{,}000$ g/mol, g'_H and g monotonically decrease with increasing MW, indicating that the larger the molecules, the more they are branched. This finding is consistent with the kinetics of free radical polymerization according to which the probability of branching by chain transfer to a dead polymer chain is approximately proportional to the chain length.[14]

The LCB density of the fractions (expressed as LCB/1000 C), as measured by ^{13}C-NMR (Table II) and estimated from the GPC data [eqs. (5) to

Table II ^{13}C-NMR Branching Data for the Parent EVA and Four Selected Fractions Obtained from Isothermal Increasing Pressure Profiling

Branch/1000 C	Parent	Fraction #11	Fraction #14	Fraction #20	Fraction #24
Ethyl	1.95	1.8	1.95	2.0	2.6
Butyl	1.95	2.4	2.2	2.0	2.0
Amyl	0.9	0.6	0.55	0.65	0.65
Hexyl+	1.8	1.8	1.1	1.35	1.35

(8)], are shown as a function of $\log_{10}(M_w)$ in Figure 11. As reported also by Mirabella and Wild,[19] the NMR data indicate little variation in LCB density across the MW range. It is known that the LCB density obtained from NMR can be overestimated because all branches with six or more carbon atoms are counted as LCBs, including chain ends. Rudin et al.[18] found that a LCB has a minimum length between 6 and 16 carbon atoms. The GPC results, on the other hand, indicate that both LCB/1000 C and LCB/molecule n_w monotonically increase with increasing M_w above 60,000 g/mol, as expected from the kinetics of free radical polymerization. Considering the broad residence time distribution characteristic of multistage HP-autoclave reactors and the steep increase in long-chain branching typically observed with increasing residence time and conversion in those reactors,[16] the small amount (<10 wt %) of high MW highly branched (>1 LCB/1000 C) material identified in this polymer [see the cumulative LCB distribution in Fig. 8(D)] corresponds most probably to those molecules that have spent an unusually long time in the reactor.

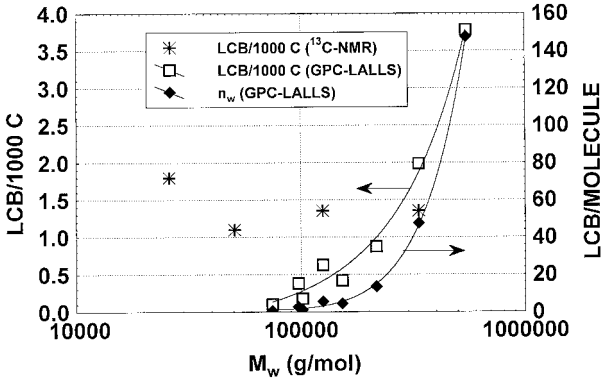

Figure 11 The LCB density (expressed as LCB/1000 C), as measured by ^{13}C-NMR and estimated from eq. (8), and the LCB/molecule (n_w) estimated from eqs. (5) to (7) using the GPC data, shown as a function of $\log_{10}(M_w)$ for a few selected fractions obtained by isothermal increasing pressure profiling.

EVA Fractionation by CITREF™

Fractionation of EVA by CITREF™ was performed in supercritical propylene at a constant pressure of ~ 612 bar, as related earlier. The acetate, alkyl, and total branch density (expressed as the number of branches per 1000 total carbon atoms) of the fourteen CITREF™ fractions collected are shown as a function of the elution temperature in Figure 12. The data show that there is a small monotonic decrease (by 10%) in acetate branch density with increasing elution temperature; the alkyl-branch density also decreases with temperature up to 46°C and increases slightly again at higher elution temperatures, as is seen with the last two fractions. The total branch density thus decreases by a total of 18% from 66.6 branches/1000 C at −1°C to 54.8 branches/1000 C at 54°C. The drop in total branch density (determined by ^{1}H-NMR) with increasing elution temperature is consistent with the concomitant increase in crystallinity and average enthalpy determined independently by DSC, which is shown in Figure 13. The benchmark used in the calculation of the percentage crystallinity is a single poly-

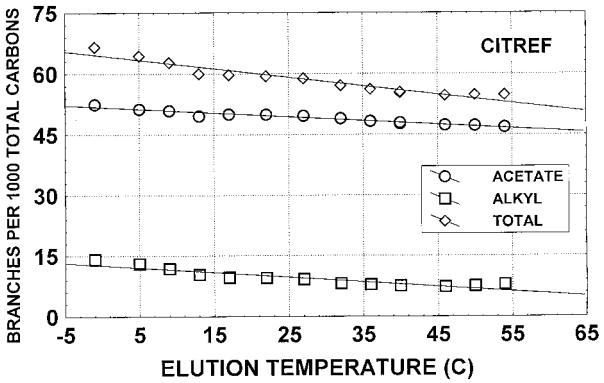

Figure 12 Number of branches per 1000 total carbons as measured by ^{1}H-NMR shown as a function of the elution temperature. CITREF™ was performed in supercritical propylene at a constant pressure of ~ 612 bar.

ethylene crystal with an enthalpy of fusion (ΔH_f^o) equal to 293 J/g (=100% crystallinity).[20] The fact that EVA crystallinity, hence, melting temperature, decreases with increasing alkyl SCB and acetate branch density represents the basis for fractionation of homo- and copolymers by CITREF™, as well as by TREF.[6,7] Indeed, it is well known that the presence of noncrystallizable copolymerized units and SCBs inhibit the formation of polyethylene crystallites.[6,7] The following relationship between the melting temperature of the fully crystalline polymer (T_m^0) and that of the semicrystalline polymer (T_m) was suggested by Flory as follows[21]:

$$\frac{1}{T_m} - \frac{1}{T_m^0} = -\left(\frac{R}{\Delta H_f^u}\right) \ln N_A \qquad (9)$$

where ΔH_f^u is the enthalpy of fusion per repeat unit; N_A is the mole fraction of crystallizable units; and R is the ideal gas constant. Note that the crystallinity of EVA approaches zero when the VA content is $\sim$ 20 mol %.

Shown in Figure 14 are T_m, determined by DSC, and the CITREF™ dissolution temperature T_m^{sol}, plotted against the total branch density. The difference in temperature between the two phase transitions is the so-called polymer melting point depression, which results essentially from the presence of dissolved propylene in the amorphous (liquid-like) domains of the semicrystalline polymer. The melting point depression for a polymer containing dissolved solvent is also given by Flory[21] as

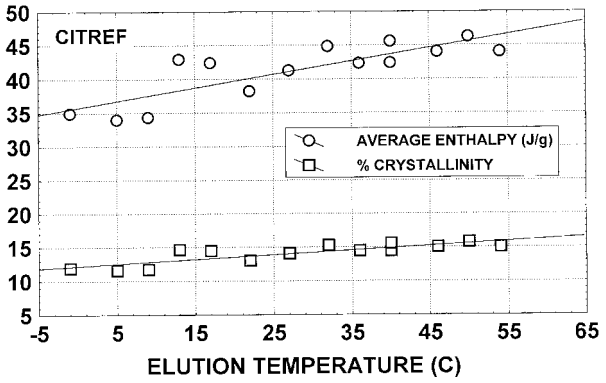

Figure 13 The average enthalpy, obtained by averaging the enthalpy of crystallization and the enthalpy of the second melting, and the percentage crystallinity shown as a function of the elution temperature for the fractions obtained by CITREF™.

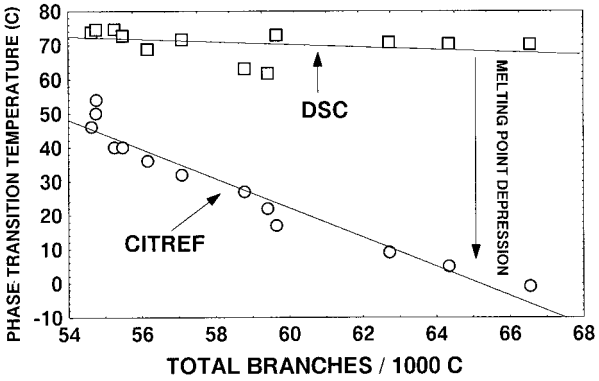

Figure 14 Phase transition temperatures versus the total branch density for the CITREF™ fractions. The empty squares represent the polymer melting temperature T_m determined by DSC. The empty circles represent the polymer dissolution temperature T_m^{sol} in propylene at 612 bar. The difference between the two phase transition temperatures is the so-called melting point depression.

$$\frac{1}{T_m^{sol}} - \frac{1}{T_m} = \left(\frac{R}{\Delta H_f^u}\right)\left(\frac{V_u}{V_1}\right)(\nu_1 - \chi\nu_1^2) \qquad (10)$$

where V_u is the molar volume of the polymer repeat unit; V_1 is the molar volume of the solvent; ν_1 is the volume fraction of the solvent dissolved; and χ is the interaction parameter. Note that as ΔH_f^u decreases (the total branch density increases), eq. (10) predicts an increase in the melting point depression, which is precisely what is shown by the data of Figure 14. The DSC crystallization curves for five selected fractions obtained from the CITREF™ run are compared to that obtained for the parent EVA in Figure 15. From Fraction #1 to Fraction #7, the curve peak shifts towards higher temperatures, indicating again that the crystallization temperature (T_c) increases with increasing elution temperature.

As clearly indicated in Figure 16(A), the alkyl branch density increases concomitantly with the acetate branch density in the CITREF™ fractions. This implies that, with propylene as the solvent, CITREF™ fractionates the polymer based on total crystallinity, which is influenced by both alkyl SCBs and acetate branches. The cumulative weight distributions for the total branch density, and separately for the alkyl and acetate branch density, are shown in Figures 16(B)–(D), respectively. Note that the difference in acetate branch density between the first and the last fraction is about 10%, suggesting that

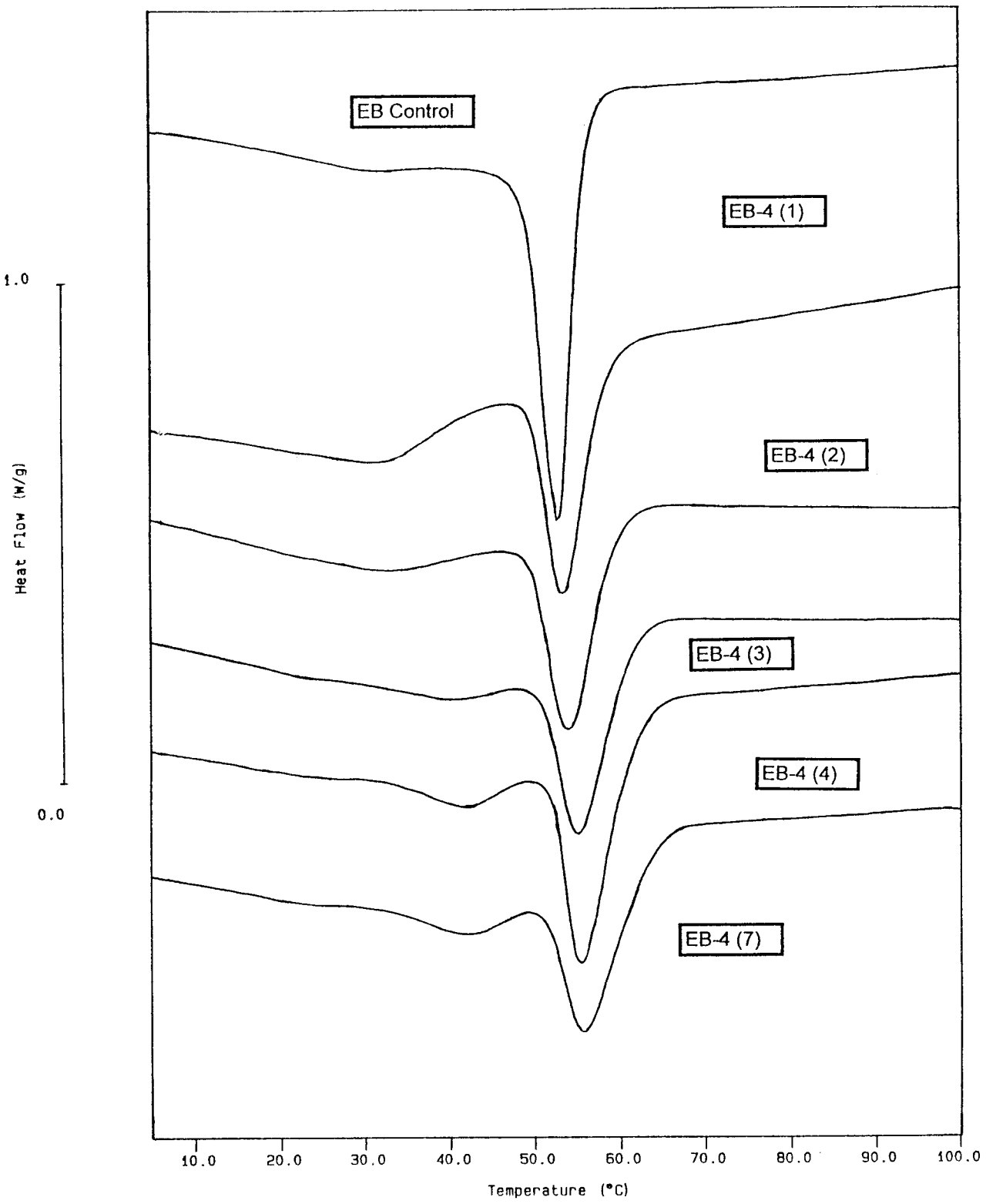

Figure 15 Superimposed DSC crystallization curves for five selected fractions obtained from CITREF™ and the parent EVA (labeled control).

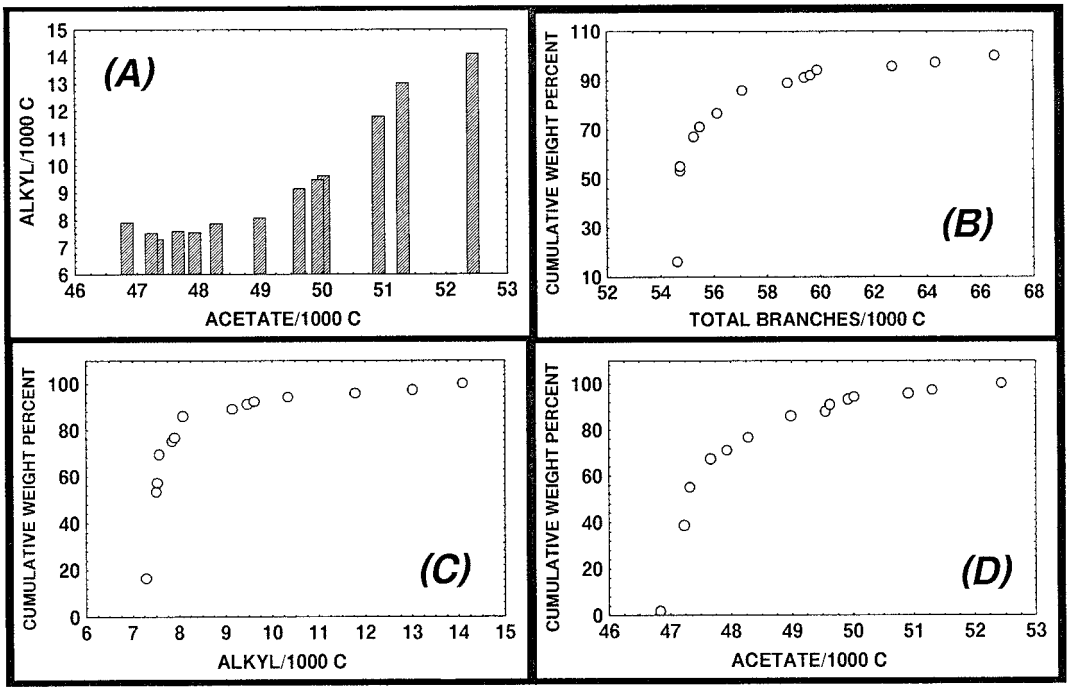

Figure 16 (A) Relationship between the alkyl branch density and the acetate branch density in the fractions collected by CITREF™. The cumulative weight distributions reconstructed from the fractions obtained by CITREF™ for (B) the total branch density, (C) the alkyl branch density, and (D) the acetate branch density.

small but significant differences in chemical composition exist between EVA molecules. Although those differences in chemical composition are not seen by the isothermal increasing pressure profiling method, they can be clearly and reproducibly identified using CITREF™.

CONCLUSIONS

A commercial HP-EVA was fractionated in supercritical propylene by isothermal increasing pressure profiling and CITREF™. The former method resulted in fractions of increasing MW and increasing LCB density, and the latter in fractions of decreasing crystallinity, resulting from a concomitant increase in both the alkyl SCB density and the acetate branch density. The in-depth characterization of the fractions performed in this work resulted in a more fundamental understanding of the molecular architecture of that complex macromolecule and provided new insights on the kinetics of free radical polymerization at high pressure.

The authors acknowledge Bernard Leroy, Rita Van de Vyver, and Jean-Jacques Muls for carrying out the polymer characterization experiments, and Dr. F. Chambon and Dr. A. Faldi for helpful technical discussions about this work. A preliminary account of this work was presented at the AIChE National Meeting (Nov. 11–15, 1996) in Chicago.

REFERENCES

1. M. A. McHugh, V. J. Krukonis, and J. A. Pratt, *Trends Polym. Sci.,* **2,** 301 (1994).
2. M. A. McHugh and V. J. Krukonis, in *Supercritical Fluid Extraction: Principles and Practice,* 2nd ed., Butterworths, Boston, 1993.
3. W. M. Saltzman, N. F. Sheppard, M. A. McHugh, R. B. Dause, J. A. Pratt, and A. M. Dodrill, *J. Appl. Polym. Sci.,* **48,** 1493 (1993).
4. J. A. Pratt, S-H. Lee, and M. A. McHugh, *J. Appl. Polym. Sci.,* **49,** 953 (1993).
5. M. A. McHugh, in *Supercritical Fluids—Fundamentals for Application,* NATO ASI Series E, Kluwer Academic, 1994.
6. P. Ehrlich, in *Supercritical Fluid—Crystal Phase Fractionation of Polymers: Polyethylene–Propane,* SUNY/Buffalo Report to National Science Foundation, Contr. CTS 8900122, Oct. 1991.

7. J. J. Watkins, V. J. Krukonis, P. D. Condo, D. Pradhan, and P. Ehrlich, *J. Supercrit. Fluids,* **4,** 24 (1991).
8. B. Folie and M. Radosz, *I&EC Res.,* **34,** 1501 (1995).
9. J. C. Randall, C. J. Ruff, M. Kelchtermans, and B. H. Gregory, *Macromolecules,* **25,** 2624 (1992).
10. Dr. A. Faldi, Private Commun., Exxon Chemical Co., Baytown Polymer Center, Baytown, TX, 1995.
11. B. Folie, *AICH J.,* **42,** 3466 (1996).
12. L. Wild, T. R. Ryle, D. C. Knobeloch, and I. R. Peat, *J. Polym. Sci., Polym. Phys.,* **20,** 441 (1982).
13. K. Shirayama, T. Okada, and S-I. Kita, *J. Polym. Sci. A,* **3,** 907 (1965).
14. P. Ehrlich and G. A. Mortimer, *Adv. Polym. Sci.,* **2,** 386 (1970).
15. W. H. Stockmayer, *J. Chem. Phys.,* **13** (6), 199 (1945).
16. P. Feucht, B. Tilger, and G. Luft, *Chem. Eng. Sci.,* **40,** 1935 (1985).
17. B. H. Zimm and W. H. Stockmayer, *J. Chem. Phys.,* **17,** 1301 (1949).
18. A. Rudin, V. Grinshpun, and K. F. O'Driscoll, *J. Liq. Chromat.,* **7,** 1809 (1984).
19. F. M. Mirabella and L. Wild, in *Polymer Characterization,* Advances in Chemistry Series 227, C. D. Craver and T. Provder, Eds., American Chemical Society, Washington, D.C., 1990.
20. J. Brandrup and E. H. Immergut, in *Polymer Handbook,* 3rd ed., Wiley, New York, 1994.
21. P. J. Flory, in *Principles of Polymer Chemistry,* Cornell University Press, Ithaca, 1983.